Available online at www.sciencedirect.com
ScienceDirect
Journal of Molecular Structure 828 (2007) 102–110
Journal of MOLECULAR STRUCTURE
www.elsevier.com/locate/molstruc

Vapor complexation in the ACl–$CrCl_3$ (A = Li, Cs) system up to 1400 K and the tetrahedral ligand field states of chromium (III)

G.N. Papatheodorou *

Foundation for Research and Technology, Hellas, Institute of Chemical Engineering and High Temperature Chemical Processes – FORTH/ICE-HT, P.O. Box 1414, GR-26504 Patras, Greece
Department of Chemical Engineering, University of Patras, GR-26504 Patras, Greece

Received 13 April 2006; received in revised form 24 May 2006; accepted 24 May 2006
Available online 14 July 2006

Abstract

Electronic absorption spectroscopy is used in the temperature range 800–1400 K, to study the vapor species, over molten $CrCl_3$–ACl (A = Li, Cs) mixtures and solid $CrCl_3$. The observed Vis/near IR bands are assigned to d ← d transitions of Cr^{3+} in distorted "tetrahedral" coordination ($CrCl_4^-$). Spectra of "octahedral" $CrCl_6^{3-}$ in molten alkali chlorides were also measured and used to estimate the spectroscopic constants (Dq, *B*, *C*) of Cr^{3+} in all chloride tetrahedral and octahedral environments. Composition and temperature-dependent measurements suggest that the predominant vapor species is the 1:1 monomer $ACrCl_4$ and that an equilibrium is established:

$$ACrCl_4\ (g) \leftrightarrows CrCl_3\ (g) + ACl\ (g)$$

Due to vapor complexation the apparent vapor pressure of $CrCl_3$ increases. The volatility enhancement is higher for the LiCl–$CrCl_3$ than the CsCl–$CrCl_3$ system reaching values near 60, at ~950 K. Based on the preferential octahedral ligand field stabilization energy of Cr(III) it is argued that dimeric and/or trimeric 1:1 species may be also present as minor components in the vapor phase. Finally, the vapor complexation and volatility enhancement for the MX_3–AX (M = rare earth, Cr; X = halide) systems are discussed and correlated to the melt structure of the corresponding binary melts.

Keywords: Vapor complexes; Electronic absorption spectra; Tetrahedral Cr(III); Vapor and melt structure

1. Introduction

Metal halide vapors and vapor complexes are important for a variety of applications including chemical synthesis and separations, extractive metallurgy and high efficiency lamps [1]. Mixtures of rare earth halides (mainly iodides and bromides) with alkali halides are used in the high temperature metal halide lamps where the formation of vapor complex species according to the reaction:

$$AX(s/l) + LnX_3(s/l) \leftrightarrows ALnX_4(g) \quad (1)$$

(A = alkali metal; Ln = rare earth; X = halide) leads to an enhancement of the apparent volatility of LnX_3 [2,3] which in turn increases the lamp spectral efficiency and decreases the required operational temperature.

The formation of the $ALnX_4$ as the predominant vapor species as well as other polynuclear in A and/or Ln vapor species is mainly verified by mass spectrometric studies [2,4,5] where the stoichiometry and the thermodynamic function can be established but no structural information can be obtained. For certain lanthanides possessing hypersensitive f ← f transitions some indirect structural information for the vapor species can also be obtained [2]. It is generally accepted [4] that the $ALnX_4$(g) is the predominant vapor species over molten AX–LnX_3 mixtures, composed of LnX_4 "tetrahedra" having the A "cation"

* Tel.: +30 6946465554; fax: +30 2610990987.
E-mail address: gpap@iceht.forth.gr

0022-2860/$ - see front matter © 2007 Published by Elsevier B.V.
doi:10.1016/j.molstruc.2006.05.041

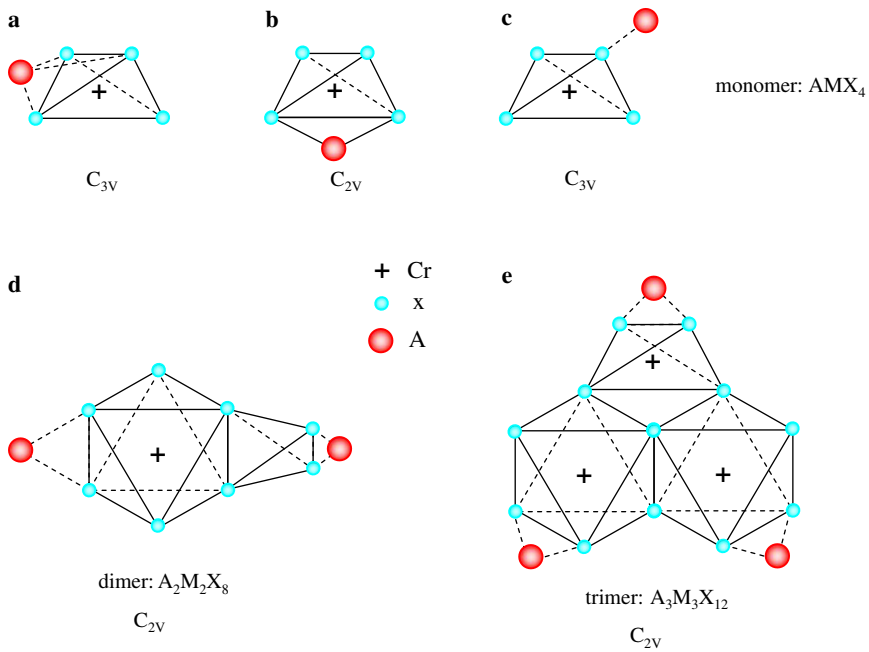

Fig. 1. Molecular models of monomeric AMX_4; dimeric $A_2M_4X_8$ and trimeric $A_3M_3X_{12}$ species. For the trimer two other model structures having the polyhedra on line can be formed; in all trimers the ratio of "octahedra" versus "tetrahedra" is 2:1.

bound to an edge or a face or a corner (Fig. 1a–c). Recent theoretical studies of $ALnX_4$ vapor species give a better inside on the structure of these molecules whose stability depends on both the size of the trivalent metal and the alkali metal [6,7]. However, no direct spectroscopic/structural information (e.g., Raman spectroscopy [3]) is available due to experimental difficulties arising from the high temperatures needed and the lack of signal intensity due to the low partial pressures of the vapor complexes.

The present work is aimed to understanding the structure of the vapor complexes formed over $AX–LnX_3$ mixtures. The rare earth cation Ln^{3+} is substituted by Cr^{3+} which is known to have d ← d ligand field sensitive electronic spectra and the vapor complexation over $LiCl–CrCl_3$ and $CsCl–CrCl_3$ mixtures is investigated by absorption spectrophotometry. The measured spectra are reasonably assigned to an all chloride "tetrahedrally" coordinated Cr(III) and are rather unique since no other "tetrahedral" d ← d spectra of Cr(III) have been reported so far in the literature. Furthermore, for purposes of comparison and in order to estimate the Cr(III) spectroscopic constants we have measured the spectra of "octahedrally" coordinated Cr(III) in an all chloride environment at elevated temperatures using molten alkali chlorides solvents.

2. Experimental

A Perkin-Elmer (Model L-900) NIR-Vis-UV spectrophotometer with reverse optics and an optical fibers attachment was used. A three zone split cylindrical furnace (50 cm long) containing an inconel metal block (20 cm long) was used for heating the long path length optical cells (10 cm) up to 1400 K. The spectrophotometer optical fibers were aligned so to focus at the center of the furnace where the optical cell was placed. Due to the absorption by the optical fibers the spectra measured with this system covered the region ~900–220 nm. For measuring the spectra in the near IR region (2000–900 nm) another smaller optical furnace was constructed. The furnace was water cooled and adjusted to fit in the spectrophotometer compartment but it could be used only for square optical cells (maximum 1 cm path length). The same furnace was used for the spectrophotometric measurements in molten alkali chlorides. Details of the constructed systems can be found elsewhere [8,9].

Chromium (III) chloride was prepared by first dehydrating commercial $CrCl_3 \cdot 6H_2O$ in a stream of gaseous HCl/N_2 at temperatures from ~700 to ~900 K. The so obtained bright purple powderous material was sublimed in sealed and evacuated fused silica tubes at 1100 K giving deep purple crystalline flakes. Anhydrous LiCl and CsCl were dried and purified by distillation at ~1000 K under dynamic high vacuum (~10^{-8} Torr). The procedures for filling up the fused silica optical cells and for measuring absorption spectra of vapor species at high temperatures have been described before [8]. All operations were carried out in an argon gas filled glove box or/and in sealed glass containers.

Table 1 lists the characteristics of the experiments performed for the vapor species. Measurements were started at ~850 K and the temperature was gradually increased in steps of 30–50 K. The quoted temperatures for the experiments with the 10 cm path length are at the center of the cell where the condensed phases were vapor transported and in most cases are about 10 K lower than those

Table 1
Characteristics of the spectrophotometric experiments

Experiment[a]	System and composition	Cell constants[b]	Moles of $CrCl_3$	t_{max}/t_{min} (K)	Volatility enhancement ρ (K)[c]
E-1	$CrCl_3$	29/10	1.28×10^{-4}	1250/900	
E-2	$CsCl–CrCl_3$ 1:1	29.5/10	1.2×10^{-4}	1260/900	15 (1050) 12 (1000) 9.5 (970)
E-3	$CsCl–CrCl_3$ 1:1	28.5/10	1.3×10^{-4}	1370/1070	0.08 (1130) 0.06 (950)
E-4	$LiCl–CrCl_3$ 1:1	27.5/10	1.18×10^{-4}	1270/910	7 (1080) 16 (1030) 45 (980) 59 (940)
E-5	$LiCl–CrCl_3$ 1:1	29/10	Excess	1120/900	
E-6[d]	$LiCl–CrCl_3$ 1:1	8.5/1	Excess	1070/1000	
E-7	$LiCl–CrCl_3$ 2:1	17/10	0.7×10^{-4}	1280/900	11 (1080) 23 (1020) 37 (950)
E-8	$LiCl–CrCl_3$ 3:1	28.5/10	1.1×10^{-4}	1370/900	9 (1080) 24 (1020) 34 (950)

[a] For all experiments the spectral range was from 850 to 220 nm except for E-6 where the range was from 2400 to 220 nm.
[b] The numbers are: volume in cm^3/path length in cm.
[c] Volatility enhancement ρ and in parentheses the corresponding temperature in K.
[d] Measurement without the fiber optics system.

of the cell windows. The spectrophotometer absorbance range for measurements with reasonable signal/noise ratio was between 0.05 and 2. The procedures for measuring the absorption spectra and molar absorptivities of Cr(III) in molten CsCl, LiCl and LiCl–KCl eutectic were the same as before [9].

3. Results and discussion

3.1. Spectra over molten LiCl–$CrCl_3$

By combining absorbance measurement from the 1 cm and the 10 cm path length cells (experiments E-4 and E-6, Table 1) we were able to measure the spectra of the vapors over the 1:1 LiCl–$CrCl_3$ mixture from 2000 to 220 nm (5000–45,000 cm^{-1}). In E-4 all the salts placed in the cell were in the vapor phase at temperatures above ~1000 K giving an almost constant absorbance at higher temperatures. This permitted the evaluation of the molar absorptivity ε (in L mol^{-1} cm^{-1}) for the vapor species formed in the LiCl–$CrCl_3$ system (Fig. 2). The energies of the observed bands are listed in Table 2. Possible assignments as well as the effect of temperature on the spectra are presented in the following subsections.

Experiment E-6 contained excess of the 1:1 mixture and thus, the absorbance was measured over the melt from ~880 to near 1070 K where optical saturation occurred due to the high concentration of the absorbing species. These measurements in combination with the molar absorptivity values permitted for each temperature the calculation of the vapor complex "apparent" partial pressure P_C and the volatility enhancement [2,3] ratio:

$$\rho = P_C/P_{CrCl_3}, \quad (2)$$

where P_{CrCl_3} is the vapor pressure over $CrCl_3$ solid [10] at the same temperature. Values of ρ are listed in Table 1.

3.2. Spectra over solid $CrCl_3$

Spectra measured in experiment E-1 at ~950 K show a strong charge transfer (CT) band in the UV region (Fig. 3a). The tale of a rather weak band (marked as T) is also present in the region of ~12,000 cm^{-1} where absorption measurements started with the fiber optics system. The presence of this band is better documented in Fig. 4a for the 1120 K spectra. At temperatures above 1200 K all the $CrCl_3$ in E-1 was vaporized and the only band observed was at 13,200 cm^{-1} (marked as C in Figs. 3a and 4a). Due to optical saturation no CT band(s) could be measured at these temperatures. Temperature-dependent measurements shown in Fig. 4a indicate an isosbestic point and a decrease of the intensity in the region of the T band.

The thermodynamic functions of vaporization of $CrCl_3$ have been measured over the years and critically evaluated [10]. Monomeric $CrCl_3$(g) and dimeric Cr_2Cl_6(g) are formed, while partial decomposition leads to the simultaneous appearance of $CrCl_4$(g) [11]. At temperatures above 1200 K the main vapor species is the monomer thus band C at ~13,200 cm^{-1} is assigned to a d ← d transition of Cr(III) in the trigonal or pyramidal $CrCl_3$ molecule.

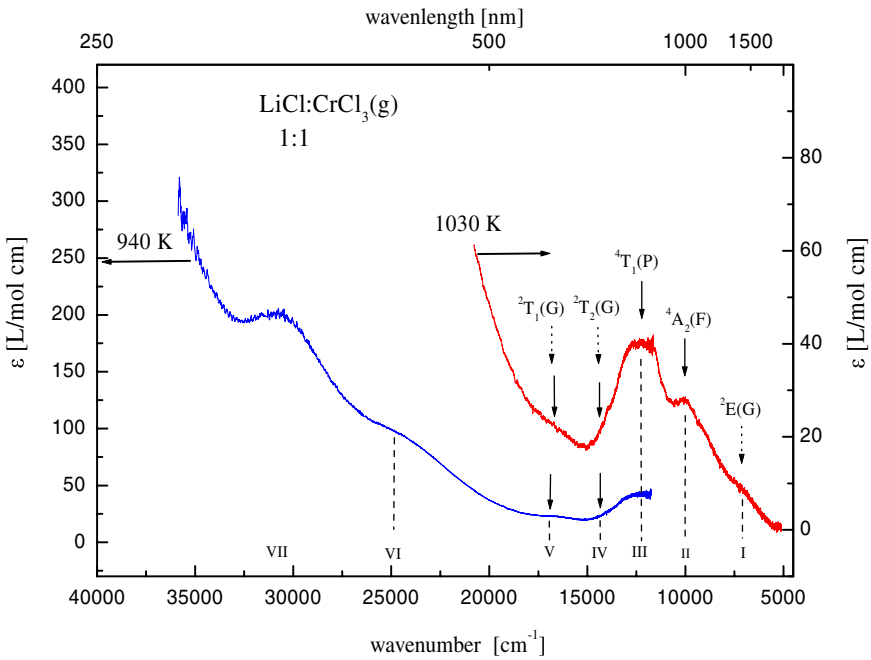

Fig. 2. Electronic absorption spectra of the vapors over LiCl–$CrCl_3$. The band positions are shown by Latin numerals on the lower part of the figure. On the upper part of the figure the vertical arrows attached to the spectroscopic symbols indicate the position of the Cr^{3+} ligand field states in tetrahedral [$^4T_1$ (F) ground state] chloride environments.

Table 2
Observed bands for Cr(III) vapor species

Band[a]	Energy (cm^{-1})	ε[b]
LiCl/$CrCl_3$ (1030 K)		
I	(7500)[c]	(10)
II	10,000	30
III	12,500	41
IV-β	(14,000)	
V-α	(16,500)	
VI	24,000	90
VII[d]	31,000	200
CsCl/$CrCl_3$ (1050 K)		
III	~12,500	~40
V-α	(16,500)	
IV-β	(14,000)	
VI	27,000	220
$CrCl_3$ (1250 K)		
T[e]	(~12,000)	
C[f]	13,200	(~13.5)
β[g]	(14,000)	
c[g]	(16,500)	
CT-1	26,000	1370
CT-2[d]	35,000	2500

[a] As marked in spectra Figs. 1–3.
[b] Approximate value of molar absorptivity in L mol^{-1} cm^{-1}.
[c] Parentheses indicate shoulder or/and weak band.
[d] Measured but not shown in spectra figures.
[e] Not well detected; assigned to the "tetrahedral" T_1(P) band of the dimer Cr_2Cl_6.
[f] Assigned to the monomer $CrCl_3$; more likely an $^4A_1(F) \leftarrow {}^4A_1(P)$, $^4E(P)$ transition in D_{3h} symmetry.
[g] Seen at low temperatures; assigned to the "tetrahedral" $^2T_1(G)$, $^2T_2(G)$ transitions of the dimer.

The Cr_2Cl_6 dimer is presumably of the Al_2Cl_6(g) type composed of edge bridged "$CrCl_4$" tetrahedra and having an absorption band (T) which is near to that of the Li–Cr–Cl "tetrahedral" complex. Thus the temperature-induced changes seen in the spectra of Fig. 4a could be considered as an indication that the vapors over $CrCl_3$ are predominated by dimer–monomer equilibrium:

$$Cr_2Cl_6(g) \leftrightarrows 2CrCl_3(g) \quad (3)$$

3.3. Spectra over molten CsCl–$CrCl_3$ and temperature effects

At low temperatures (<950 K) and in the region 850–500 nm (~11,500–20,000 cm^{-1}) the spectra over molten CsCl–$CrCl_3$ (1:1 and 1:3) measured in experiments E-2 and E-3 (Figs. 3b and 5a) are very similar to those of LiCl–$CrCl_3$ (1:1, 1:2 and 1:3) (Figs. 4b and 5b). The molar absorptivities in the region around 12,000 cm^{-1} are also close but the near UV spectra show marked differences. Measurements over excess CsCl–$CrCl_3$ liquid mixtures show that the volatility due to vapor complexation is somewhat lower than that of the LiCl–$CrCl_3$ system (Table 1).

In experiments E-2 and E-3, all condensed phases were evaporated at ~950 K. By gradually increasing the temperature the ~12,000 cm^{-1} band shifted to the blue reaching at 1250 K an energy close to the 13,200 cm^{-1} which corresponds to the C band of the $CrCl_3$ monomer (Figs. 3b and 5a). This would imply that an equilibrium is established where the Cs–Cr–Cl vapor complex dissociates to $CrCl_3$ and CsCl. Assuming that the vapor complex is a monomer with 1:1 stoichiometry then the temperature

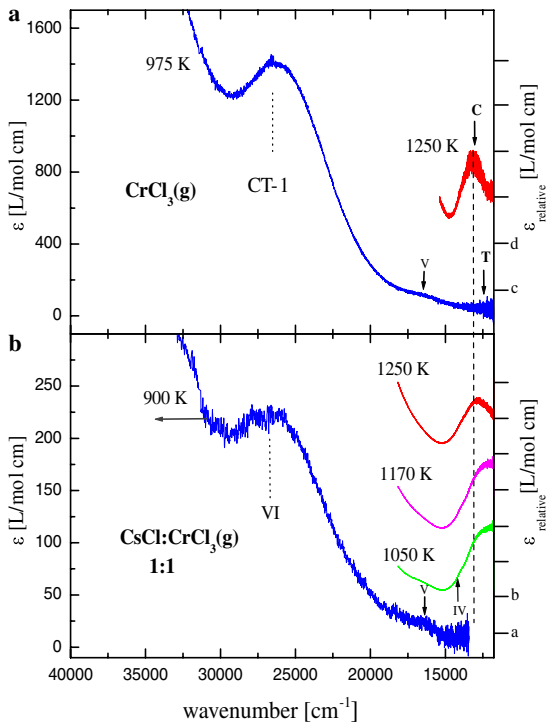

Fig. 3. Electronic absorption spectra of vapors over solid $CrCl_3$ and molten CsCl–$CrCl_3$ mixture. (a) At 975 K the spectra on the left are predominated by the CT transitions in the equilibrium vapor mixture $CrCl_3$–Cr_2Cl_6; at 1250 K band C of the spectra on the right corresponds to a $d \leftarrow d$ transition of Cr^{3+} in a trigonal field. No baseline could be established for the spectra but the molar absorptivity can be estimated from the magnitude of the scale: dc = 10 L mol^{-1} cm^{-1}. (b) Vapors over CsCl–$CrCl_3$ (1:1) melt; with increasing temperature band C due to $CrCl_3$ (g) appears in the spectra suggesting the dissociation reaction (4); the molar absorptivity can be estimated from the magnitude of the scale: ab = 10 L mol^{-1} cm^{-1}.

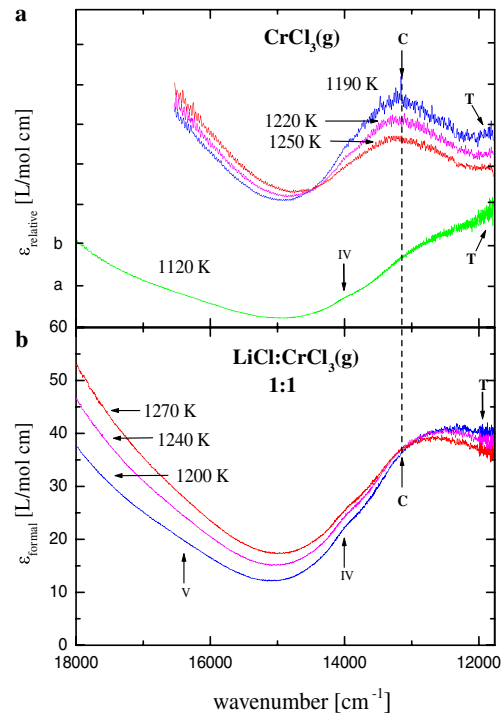

Fig. 4. Temperature dependence of the electronic absorption spectra. (a) Chromium (III) chloride vapors; the relative change of the T to C bands and the isosbestic point suggest a dimer–monomer equilibrium; absorptivities can be estimated from the magnitude of the scale: ab = 10 L mol^{-1} cm^{-1}. (b) The LiCl–$CrCl_3$ (1:1) vapors; the isosbestic point and the appearance of the C band of $CrCl_3$(g) suggest the dissociation reaction (5).

dependence of the spectra in Figs. 3b and 5a suggests the dissociation:

$$CsCrCl_4(g) \leftrightarrows CsCl(g) + CrCl_3(g) \quad (4)$$

In support of this dissociation is the analogous behavior of the Li–Cr–Cl vapor complex spectra at high temperatures as seen in Figs. 4b and 5b. The intensity of the 12,000 cm^{-1} band decreases with increasing temperature, a blue shift occurs towards the C band of $CrCl_3$ (g) in the spectra of both the 1:1 and 1:3 compositions. This accounts as above for the dissociation:

$$LiCrCl_4(g) \leftrightarrows LiCl(g) + CrCl_3(g) \quad (5)$$

In other words it appears that the spectral behaviors of the vapor complexes formed in the ACl–$CrCl_3$ (A = Li, Cs) systems are similar suggesting that species of the same stoichiometry are formed which at high temperatures dissociate.

3.4. Melt structure and vapor complexation

Many molten binary systems of the type AX–MX_3 (M = rare earth, group 3B, etc.) have been investigated by different physicochemical methods. Thermodynamic [12,13] and Raman spectroscopic [14,15] studies have shown that these mixtures are stabilized by forming associated ("complex") species. For trivalent cations with relatively "large" ionic radii (M = Y, ..., La) the MX_6^{3-} octahedra predominate the melt structure and stabilize the AX-rich melts while for much smaller sizes (M = Al, Fe) the main species formed are the MCl_4^- tetrahedra. For intermediate size cations (e.g., Sc) the melt structure for compositions $0.3 < x < 0.6$ (x = mole fraction of the trivalent halide) involves both the "octahedral" and the "tetrahedral" species [16,17]. At $x = 0.25$ the "octahedra" predominate the structure while the maximum concentration of the "tetrahedra" is found in equilibrium with "octahedra" at $x = 0.5$. The formation and stability of the "complex" species (MCl_4^-, MX_6^{3-}) in the melt mixtures is also affected by the alkali metal cation A^+ and has been found to change systematically from Li to Cs. For the LiX–MX_3 melts both the MCl_4^- and MX_6^{3-} species are strongly distorted from the high ionic potential of the neighboring Li^+ and possess short life times and lower thermodynamic stability relative to the CsX–MX_3 melts.

The data in Table 1 are in accordance with the above behavior showing that the volatility enhancement of the less stabilized LiCl–$CrCl_3$ melts is higher than that of the CsCl–$CrCl_3$ melts. Furthermore, by increasing the

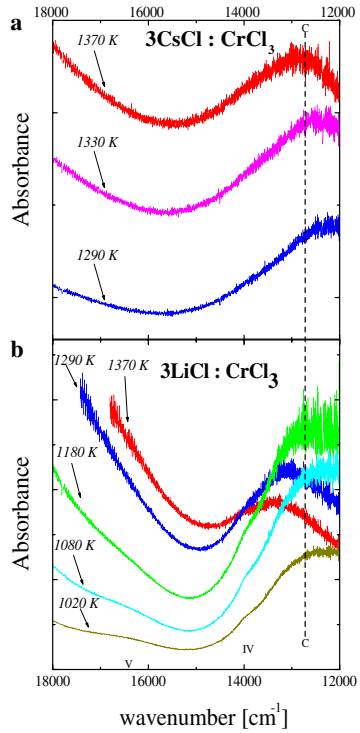

Fig. 5. Temperature dependence of the electronic absorption spectra (a) the Cs–Cl–$CrCl_3$ (1:3) vapors and (b) the LiCl–$CrCl_3$ (1:3) vapors. In both systems increasing temperature gives rise to the C band of the $CrCl_3$ monomer.

ACl–$CrCl_3$ ratio from 1:1 to 1:2 to 1:3 the volatility enhancement decreases which would also imply that the ACl-rich melts are rather stable mixtures as expected from the formation of the $CrCl_6^{3-}$ "complexes" in these melts. The ionic radii ratio Cr^{3+}/Cl^- is close to that of Sc^{3+}/I^- thus the CsCl–$CrCl_3$ melt structure is more likely to be similar to that of CsI–ScI_3 and to some extent to the CsCl–$ScCl_3$ melts [16,17]; this without taking into account the strong d-electron octahedral ligand field stabilization energy (LFSE) of Cr(III) (for ligand field effects see, e.g., Refs. [18–20] for solids and Ref. [12] for melts). For the 1:3 composition ($x = 0.25$) the formation of $CrCl_6^{3-}$ is expected to further stabilize the melt by the high octahedral LFSE of Cr(III) thus vaporization to a species not having octahedral coordination requires higher enthalpy relative to melts involving trivalent ions without d-electrons (e.g., Y, Sc). On the other hand for the 1:1 composition both the $CrCl_6^{3-}$ and $CrCl_4^-$ species are expected to coexist as in the case of the CsX–ScX_3 melts [16,17]. Thus vaporization of the 1:1 melt to species having the Cr(III) in tetrahedral coordination is facilitated from the existence of $CrCl_4^-$ ions in the melt and the phase transition is not inhibited by the LFSE effects. This would imply that the most probable 1:1 vapor species contains the $CrCl_4$ "tetrahedra". The presence of such a species supports the assumption used for interpreting the vaporization data of many AX–MX_3 systems by means of AMX_4(g) vapor molecules [2–5].

Apart from composition the volatility enhancement depends also on temperature (Table 1). For the LiCl–$CrCl_3$ system the highest enhancement occurs for the 1:1 melts at the lowest temperature but at the highest temperature studied (~1100 K) the same values are reached for all three LiCl compositions. This behavior is attributed to decomposition of the vapor complex at high temperatures (i.e., reaction (5)). Reversely, for the CsCl–$CrCl_3$ system the volatility enhancement is rather low and the values tend to increase with temperature indicating a higher stability of the chromium vapor complex relative to the free $CrCl_3$ vapor (i.e., reaction (4)). The LFSE of Cr(III) in the distorted tetrahedral field of $ACrCl_4$ and in the threefold coordination field of $CrCl_3$ presumably play an important role in determining the relative stabilities of the species involved in reactions (4) and (5).

3.5. Spectra of "octahedral" Cr(III) in molten alkali chlorides

From the Raman spectroscopic and the thermodynamic studies mentioned in the previous subsection one would expect that the dissolution of Cr(III) in alkali chloride melts should lead to the formation of $CrCl_6^{3-}$ "octahedral" species. Fig. 6 shows the absorption spectra of Cr(III) in molten LiCl, CsCl and LiCl–KCl eutectic. The assignments given in the figure are based on the similarities of the spectra to many "octahedral" Cr(III) spectra studied over the years in the solid state and in solutions (e.g., Refs. [19–21]). Table 3 gives the assignments of the eutectic

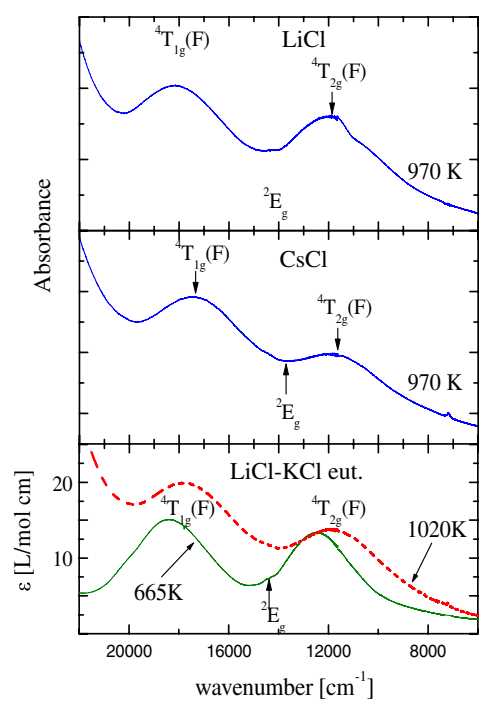

Fig. 6. Electronic absorption spectra of Cr(III) in molten alkali chloride solvents. Band assignments are bases on the $CrCl_6^{3-}$ octahedral states (Table 4). In the LiCl melts splitting due to distortions occurs.

spectra and compares the experimental values with those calculated from the Tanabe–Sugano diagrams [18]. Well-established methods for calculating from our spectra the Racah parameters B_{O_h} and C_{O_h} and the splitting parameter Dq_{O_h} were used [19].

The spectra in molten LiCl are more complicated due to the fact that the $CrCl_6^{3-}$ "octahedra" are rather distorted by the high ionic potential of the neighboring lithium anion. The distortions split the degenerate $^4T_{2g}$ (F) and $^4T_{1g}$ (F) terms giving components near and around the undistorted "octahedral" values. For all three melts the position of the spin forbidden ^2E_g(G) band remains practically unchanged due to the insensitivity of this state to the Dq_{O_h} splitting parameter as deduced from the Tanabe–Sugano diagrams. Finally, it should be noted that the molar absorptivity values of the d–d transitions are rather low ($\varepsilon < 15$ L mol^{-1} cm^{-1}, Fig. 5) as expected from the Laporte forbidden character of these transitions in "octahedral" symmetry.

3.6. Spectra of tetrahedral Cr(III) in the vapor complex and assignments

The spectra of vapors in the Li–Cr–Cl system shown in Fig. 2 possess bands at relatively low energies in comparison with the so far known spectra of Cr(III) coordinated to different inorganic ligands in solids and solutions [19–21]. Starting from the "lower" limit of our spectrophotometer (5000 cm^{-1}) and up to 20,000 cm^{-1} a set of at least five bands (marked as I–V) can be recognized in the spectra. The molar absorptivities are also higher than the values measured for the "octahedral" Cr(III) in the alkali chloride melts. These observations alone suggest that the vapor species spectra are due to d ← d chromium transitions in a rather weak ligand field. Furthermore, by taking into account that the most probable vapor species is the $LiCrCl_4$ we conclude that the spectra in Fig. 2 correspond to the" tetrahedral" chromium "$CrCl_4$" in distorted field(s) due to the presence of the neighboring Li.

The splitting parameter Dq_{T_d} of Cr(III) in an all chloride tetrahedral field can be estimated from the Dq_{O_h} of $CrCl_6^{3-}$ (Table 3) and the relation $Dq_{T_d} = 4/9\ Dq_{O_h} = 528$ cm^{-1}. The difference between the ground state of the d^3 configuration $^4T_1$(F) and the first excited state $^4T_2$(F) is 8 Dq_{T_d} which brings the $^4T_2$(F) energy of Cr(III) at ~4680 cm^{-1}, i.e., outside the spectrophotometer range. The remaining states are expected at higher energies and presumably are the bands seen in the spectra of Fig. 2. The octahedral ligand field parameters Dq_{O_h}, B_{O_h} and C_{O_h} given in Table 3 in correlation with the systematics observed for other first row transition metal ions can be used to estimate the corresponding parameters of Cr(III) in tetrahedral field. Thus from the extensive spectroscopic work on Ni(II) in different all chloride coordination geometries [22–24] the Racah parameters B and C have been calculated for both Ni(II) octahedral and tetrahedral fields. By scaling the B_{O_h} and C_{O_h} values of $CrCl_6^{3-}$ to the Ni(II) values the B_{T_d} and C_{T_d} parameters of $CrCl_4^-$ can be estimated. These parameters are listed in Table 4 along with the energy states of tetrahedral $CrCl_4^-$ which are based on the Tanabe–Sugano diagrams [18]. A comparison with the experimental date permits an assignment of all the visible and near IR bands (I–V) seen in the spectra of Fig. 2 and is listed in Table 4. As mentioned above the $^4T_1$(F) ← $^4T_2$(F) transition is predicted below the spectrophotometer limit and cannot be measured. Very good

Table 4
Assignments and calculated bands of Cr(III) in gaseous $LiCrCl_4$

$CrCl_4$ (T_d symmetry) ; Dq_{T_d} = 528 cm^{-1}; B_{T_d} = 540 cm^{-1}; C_{T_d} = 3070 cm^{-1}		
Transition [$^4T_1$(F)]→	Measured (cm^{-1})	Calculated[(a)] (cm^{-1})
$^4T_2$ (F)	–	4680
^2E (G)	(7500)[(b)]	7740
$^4A_2$ (F)	10,000	10,080
$^4T_1$ (P)	12,500	12,240
$^2T_1$ (G)	(14,000)	14,220
$^2T_2$ (G)		14,580
$^2A_1$ (G)	(16,500)	16,920

[a] Using the Tanabe-Sugano diagrams
[b] Shoulder bands are in parenthesis

Table 3
Assignments and calculated bands for Cr(III) in melts

$CrCl_6^{3-}$ (O_h symmetry)					
Molten CsCl (Cr^{3+}) Dq_{O_h} = 11,900 cm^{-1}; B_{O_h} = 580 cm^{-1}; C_{O_h} = 3310 cm^{-1}			Molten LiCl–KCl eutectic (Cr^{3+}) Dq_{O_h} = 12,500 cm^{-1}; B_{O_h} = 600 cm^{-1}; C_{O_h} = 3370 cm^{-1}		
Transition [$^4A_{2g}$(F)]→	Measured (cm^{-1})	Calculated[a] (cm^{-1})	Transition [$^4A_{2g}$(F)]→	Measured (cm^{-1})	Calculated[a] (cm^{-1})
$^4T_{2g}$ (F)	11,905	11,900	$^4T_{2g}$ (F)	12,500	12,500
^2E_g (G)	14,400	14,400	^2E_g (G)	14,400	14,500
$^4T_{1g}$ (F)	17,390	17,400	$^4T_{1g}$ (F)	18,200	18,215
$^4T_{1g}$ (P)	–	26,700	$^4T_{1g}$ (P)	–	28,071

[a] Using the Tanabe–Sugano diagrams.

agreement between experimental and calculated values is found for the spin allowed ligand field transitions arising from the ^4F and ^4P free ion states. These transitions depend only on the Dq_{T_d} and B_{T_d} parameters which confirms the correctness of the estimation of the parameters as listed in Table 4. Some disagreement, however, exists for the intercombination bands (spin forbidden states) arising from the splitting of the ^2G free ion states. The energies of the resulting $^2E(G)$, $^2T_1(G)$, $^2T_2(G)$ and $^2A_1(G)$ terms depend on the Dq_{T_d} and B_{T_d} parameters and in addition on the C_{T_d} Racah parameter which determines the overall position of the ^2G relative to ^4P and ^4F free ion states. Thus it seems that the origin of disagreement is due to inaccuracies in the estimation of the C_{T_d} parameter.

Finally, the spectra of vapors over both the $LiCl–CrCl_3$ and the $CsCl–CrCl_3$ systems show bands near the UV region marked as VI and VII (Fig. 2 and Table 2). These bands may arise from either the splitting of the higher energy ^2H, ^2P or ^2D free ion states or are related to the electron donating/accepting properties of the ligand (charge transfer bands, CT). In the first case the transitions are spin forbidden and weak bands are expected; thus with molar absorptivities higher than 100 L mol^{-1} cm^{-1} it is more likely that these high energy transitions have a charge transfer origin.

In the vapor molecule $LiCrCl_4$ the T_d symmetry of the tetrahedral is expected to be distorted by the field of the neighboring Li^+ cation. Depending on the position of Li along the edge, the face or the corner of the tetrahedra (Fig. 1a–c) the symmetry will be lowered to C_{3v} or C_{2v}. These lower symmetries should further split the degenerate tetrahedral ligand field terms to sets of component states. At elevated temperatures these components would be rather difficult to resolve in the spectra resulting broader bands centered around the energy of the degenerate tetrahedral term. The spectra in Fig. 2 support this view and show that the degenerate $^4T_1(P)$ band possesses a broader maximum and a higher half-width relative to the non-degenerate $^4A_1(F)$ band.

In conclusion the above analysis establishes for the first time the near IR/Vis ligand field states of an all chloride coordinated chromium (III) in nearly tetrahedral symmetry.

3.7. The multi-structure of the 1:1 vapor species

The above data and discussion infer that the vaporization occurs easier from the 1:1 melt and that the same stoichiometry is kept in the vapor. The absorption spectra indicate that a "tetrahedrally" coordinated Cr(III) is present in the gas phase thus the most probable vapor species is the $ACrX_4$ monomer. Such molecules have been found to be the predominant vapor species over a large number of $AX–MX_3$ molten systems [2–5]. Mass spectrometric studies have also shown that apart from AMX_4 other species like the dimers $A_2M_2X_8$ and/or the five coordinated A_2MX_5 species exist as minor components [2,5]. The structure of the monomer AMX_4 can be easily visualized from the three structural models a, b, and c in Fig. 1 and the "tetrahedral" coordination (versus, e.g., a square planar) is supported, at least for Cr(III), from the above analysis of the absorption spectra. On the other hand the most probable structural models for the dimer $A_2M_2X_8$, trimer $A_3M_3X_{12}$, etc., more likely involve mixed "tetrahedral" and "octahedral" coordinations of M(III). This is shown in Fig. 1 with examples for the dimer (d) and a trimer (e).

In the case of Cr(III) both the "octahedra" and "tetrahedra" present in the dimers (Fig. 1) should contribute to the absorption spectra of the vapors. On the other hand since the molar absorptivity of the "octahedra" is lower than that of the "tetrahedra" and since the dimers are more likely the minor components, then the absorption spectra should be dominated from the "tetrahedral" absorption bands. In other words the "tetrahedral" spectra in Fig. 2 cannot exclude the presence of more than one "tetrahedral" species in the vapor phase; i.e., both $ACrX_4$ and $A_2Cr_2X_8$ or even higher polymers may be present. This would imply that the volatility enhancements in Table 1 are underestimated.

The presence of more than one vapor species over the $ACl–CrCl_3$ systems is also supported from a thermodynamic and a LFSE (Section 3.4) point of view. The Raman spectroscopic studies in molten $CsCl–ScCl_3$ mixtures have shown that near the 1:1 composition an equilibrium takes place:

$$2Sc_2Cl_9^{3-} = 3ScCl_4^- + ScCl_6^{3-}; \quad \Delta H_{Sc} = 38 \text{ kJ mol}^{-1}, \tag{6}$$

where the dimer structure consists of two "octahedra" bound by a face [16]. The vaporization of the 1:1 melt mixture to form $CsScCl_4$ would imply that $ScCl_4^-$ leaves the melt and thus the above equilibrium should shift to the right. On the average the equilibrium transforms three "octahedra" to three "tetrahedra" and in the absence of LFSE the enthalpy of the above reaction is mainly associated to breaking the bridging bonds of the dimer and lowering the coordination. If, as discussed in Section 3.4, the structure of molten $ACl–CrCl_3$ (1:1) is similar to that of the corresponding $ScCl_3$ melts, then an analogous equilibrium (6) for the $ACl–CrCl_3$ system should be influenced by the "octahedra"/"tetrahedra" LFSE of Cr(III). From the Dq values in Tables 3 and 4 the LFSE of the two different geometries can be estimated yielding the enthalpy for the coordination change:

$$CrCl_6^{3-} = CrCl_4^- + 2Cl^-; \quad \Delta H_{LF} = 130 \text{ kJ mol}^{-1}. \tag{7}$$

And for corresponding equilibrium in the melt we may write:

$$2Cr_2Cl_9^{3-} = 3CrCl_4^- + CrCl_6^{3-};$$
$$\Delta H_{Cr} = \Delta H_{Sc} + 3\Delta H_{LF} = 430 \text{ kJ mol}^{-1}. \tag{8}$$

Thus the Cr(III) evaporation from the melt to form the 1:1 monomer $ACrCl_4$ requires that equilibrium (8) shift to the right, a process which is inhibited by the high endothermic enthalpy. On the other hand if the vaporization leads in

part to a species having also the Cr(III) in "octahedral" coordination like in molecules d and e (Fig. 1) a counterbalance of the LFSE would occur and this would make vaporization energetically more favorable for these molecules.

Thus, relative to the lanthanide chloride MCl_3–ACl system the $CrCl_3$–ACl system is expected to have a higher percentage of "polymeric" species in the vapor phase. In this respect high temperature mass spectrometric studies over ACl–$CrCl_3$ would be enlightening.

Acknowledgments

Many thanks to Ms. I. Tzianaki, Mr. D. Barkoulis and Dr. A. Kalambounias for their kind help.

References

[1] See for example: Theo. G.M.M. Kappen, in: G. Zissis (Ed.), Proceedings of the 10th International Symposium on the Science and Technology of Light Sources, Toulouse, France, 2004, p. 43 and other related papers in the same Proceedings.
[2] S. Boghosian, G.N. Papatheodorou, in: K.A. Gschneidner, L.R. Eyring (Eds.), Handbook of the Physics and Chemistry of Rare Earths, vol. 23, Elsevier, Amsterdam, 1996, p. 435.
[3] G.N. Papatheodorou, in: E. Kaldis (Ed.), Current Topics in Materials Science, vol. 10, North-Holland Publ., Amsterdam, 1982, p. 250.
[4] K. Hilpert, U. Niemann, Thermochim. Acta 299 (1997) 49.
[5] K. Hilpert, Struct. Bond. 73 (1990) 97.
[6] C.P. Groen, A. Oskam, A. Kovacs, Inorg. Chem. 39 (2000) 6001.
[7] C.P. Groen, A. Oskam, A. Kovacs, Inorg. Chem. 42 (2003) 851.
[8] A. Chrissanthopoulos, G.D. Zissi, G.N. Papatheodorou, ECS Proceedings (2006) in press.
[9] A. Chrissanthopoulos, G.N. Papatheodorou, Phys. Chem. Chem. Phys. 2 (2000) 3709.
[10] B.B. Ebbinghaus, Combust. Flame 101 (1995) 331.
[11] J.S. Ogden, R.S. Wyatt, J. Chem. Soc. Dalton Trans. (1987) 859.
[12] G.N. Papatheodorou, in: J.O. Bockris, B.E. Conway, E. Yaeger (Eds.), A Treatise of Electrochemistry, vol. 5, Plenum Press, New York, 1983, p. 339.
[13] M. Gaune-Escard, in: M. Gaune-Escard (Ed.), Molten Salts: From Fundamentals to Applications, NATO Science Series, Kluwer Academic Publishers, Dordrecht, 2002, p. 375.
[14] G.N. Papatheodorou, S.N. Yannopoulos, in: M. Gaune-Escard (Ed.), Molten Salts: From Fundamentals to Applications, NATO Science Series, Kluwer Academic Publishers, Dordrecht, 2002, p. 47.
[15] M. Brooker, G.N. Papatheodorou, in: G. Mamantov (Ed.), Advaces in Molten Salts Chemistry, vol. 5, Elsevier, Amsterdam, 1983, p. 27.
[16] M. Metallinou, L. Nalbandian, G.N. Papatheodorou, W. Voigt, H.H. Emons, Inorg. Chem. 30 (1991) 4261.
[17] G.D. Zissi, G.N. Papatheodorou, Phys. Chem. Chem. Phys. 6 (2004) 480.
[18] S. Sugano, Y. Tanabe, H. Kamimura, Multiplets of Transition-Metal Ions in Crystals, Academic Press, New York, 1970.
[19] B. Henderson, G.F. Imbusch, Optical Spectroscopy of Inorganic Solids, Clarendon Press, Oxford, 1989.
[20] For a series of reviews on ligand field spectra, see, e.g., Struct. Bond. (2004) 106.
[21] K. Hermanowicz, J. Lumin. 109 (2004) 9.
[22] J. Brynestad, H.L. Yakel, G. Pedro Smith, J. Chem. Phys. 45 (1966) 4652.
[23] T.W. Couch, G. Pedro Smith, J. Chem. Phys. 53 (1970) 1336.
[24] J. Brynestad, G. Pedro Smith, J. Am. Chem. Soc. 92 (1970) 3189.